Lab on a Chip

Dynamic Article Links

Cite this: *Lab Chip*, 2012, **12**, 3063–3072

www.rsc.org/loc

PAPER

Live cell imaging analysis of the epigenetic regulation of the human endothelial cell migration at single-cell resolution†

Chunhong Zheng,‡[a] Zhilong Yu,‡[a] Ying Zhou,‡[a] Louis Tao,[b] Yuhong Pang,[a] Tao Chen,[a] Xiannian Zhang,[a] Haiwei Qiu,[a] Hongwei Zhou,[a] Zitian Chen[ac] and Yanyi Huang*[ac]

Received 22nd February 2012, Accepted 11th April 2012
DOI: 10.1039/c2lc40192d

Epigenetic regulation plays an important role in cell migration. Although many methods have been developed to measure the motility of mammalian cells, accurate quantitative assessments of the migration speed of individual cells remain a major challenge. It is difficult for conventional scratch assays to differentiate proliferation from migration during the so-called wound-healing processes because of the long experimental time required. In addition, it is also challenging to create identical conditions for evaluating cell migration by conventional methods. We developed a microfluidic device with precisely created blanks allowing for robust and reproducible cell migration inside accurately-controlled microenvironments to study the regulatory effect of the epigenetic regulator histone deacetylase 7 (HDAC7) on cell migration. Through analyzing time-lapse imaging of the cells migrating into individual blank regions, we can measure the migration speed parameter for human primary cells within a few hours, eliminating the confounding effect of cell proliferation. We also developed an automatic image analysis and a numeric model-based data fitting to set up an integrated cell migration analysis system at single-cell resolution. Using this system, we measured the motility of primary human umbilical vein endothelial cells (HUVECs) and the migration speed reduction due to the silencing of HDAC7 and various other genes. We showed that the migration behaviour of these human primary cells are clearly regulated by epigenetic mechanisms, demonstrating the great potential of this accurate and robust assay in the fields of quantitatively migration studies and high-throughput screening.

Introduction

The migration of mammalian cells plays a critical role in many biological processes, including cancer metastasis, embryonic development, wound healing, immune response, organogenesis, and tissue regeneration.[1,2] Cell motility, one of the key factors to describe migration, has been extensively studied and used to confirm gene functions[3] and to evaluate and screen drugs.[4] Migration-related genes are connected to many biological processes and form a complex network.[5] Recent discovery has shown that epigenetic modification also critically regulates cell migration.[6] Histone deacetylases (HDACs) are a family of enzymes that modulate gene expression through the removal of an acetyl group from the lysine residue on a histone protein.[7] Several groups have shown that knockdown of HDAC7 will decrease endothelial cell (EC) migration speed.[8] However, different experiments have drawn inconsistent conclusions from the correlation between HDAC7 and cell proliferation.[8,9] Considering the strong possibility of conflating pure motion and cell division during the migration experiment, and the difficulty of reproducing the migration condition between different experimental runs, it is highly desirable to find a quantitative, robust, automated, and scalable method to evaluate migration.

The most popular method to study collective migration of cells is the wound-healing scratch assay.[10] A monolayer of cells is scratched by a fine pipette tip to create a gap, which is then allowed to "heal". The width of the "scratch" is measured as a function of time to determine the migration speed. This scratch method-produced wound reflects a natural wound and the procedure is simple and easy to set up, but it is difficult to produce precise and reproducible results. Firstly, during wound generation, it is unavoidable to damage the cells, thus interfering with motility quantification. Secondly, to obtain reliable results, the procedure usually takes 12 h or longer for cells to migrate a sufficiently long distance, during which cells can proliferate profusely, making significant contribution to wound healing.

[a]*College of Engineering, and Biodynamic Optical Imaging Center (BIOPIC), Peking University, Beijing, 100871, China. E-mail: yanyi@pku.edu.cn*
[b]*Center for Bioinformatics, National Laboratory of Protein Engineering and Plant Genetics Engineering, College of Life Sciences, Peking University, Beijing, 100871, China*
[c]*College of Chemistry and Molecular Engineering, Peking University, Beijing, 100871, China*
† Electronic supplementary information (ESI) available. See DOI: 10.1039/c2lc40192d
‡ These authors contributed equally to this work.

Thirdly, reproducibility is poor as each step has to be performed manually, making it difficult to determine whether some of the subtle changes result from human inference or system error, or from real biological effects. Finally, when increasing throughput, scratch essay experiments require large amounts of samples and reagents, making it costly to handle multiple samples simultaneously. Several modified methods, including aqueous two-phase dextran droplets surface blocking[11] and the commercially available polymeric insert mask,[12] have been developed to create a non-invasive blank inside a cell monolayer and observe the cell invasion into the blanks. These methods are good replacements for the conventional scratch assays since they offer an intuitive analogy and conventional operation to researchers. However, these approaches still require long time to allow the cells to move sufficient distances for an accurate quantification of cell motility.

Recently many groups have developed chip-based assays to realize wounding by electrical pulses,[13] trypsin digestion,[14] PDMS micro-stencil,[15] self-assembled mono-layers (SAMs),[16] surface tension,[17] micromachined plate,[18] and temperature-sensitive releasing.[19] These techniques were developed to solve the above-mentioned problems, by increasing the throughput, lowering sample consumption or improving the reproducibility. However, most of these methods cannot avoid cell or surface damage during wounding, and, by themselves, cannot differentiate cell proliferation from migration. Thus the precise and quantitative observation, recording, and analysis of cell mobility remain to be fully realized.

Here we present a novel method to quantitatively measure cell migration speed with the ability to track single-cell movement and the collective migration simultaneously, and use this method to study the epigenetic regulation of HUVEC migration. This method is a fully integrated system, consisting of a microfluidic device, a set of home-developed microscopic image acquisition and processing program, and a pair of migration calculation algorithms using both analytical model, and numerical simulations. This migration assay, using merely a few hundred to a few thousand of cells, takes only 3 to 4 h to distinguish the motility difference between differently treated cells with minimum influence of the division and great reproducibility. We also built a "particle" model and a simplified collective migration model to fit the experimental data. We found that both single-cell tracking and collective migration fitting give similar results. Knockdown of HDAC7 slows down the HUVEC migration by 25%, showing the distinct epigenetic regulatory effect on cell motility. With the ability to perform both single-cell tracking and counting, we can accurately differentiate the division change caused by knocking down HDAC7. We also examine the migration regulated by HoxA9, a crucial transcription factor which itself is epigenetically regulated by HDACs. The quantitative assessment of the regulatory effectiveness of different migration related genes could be precisely measured through this method, demonstrating the great potential of its applications in screening and evaluating functional genes and drugs.

Methods

Fabrication of blank-fill chips

We fabricated blank-fill chips by multi-layer soft lithography technology.[20,21] In brief, we first used the photolithographic process to fabricate molds for the fluidic channels and control channels. The mold of the control channels, including the button valves similar to the "MITOMI chips",[22] was made from a 20 μm negative photoresist (SU8-2010, MicroChem, Newton, MA, USA) patterned on a silicon wafer. The mold of fluidic channels was made from positive photoresist (P4620, AZ Electronic Materials, Branchburg, NJ, USA). The fluidic channel was rounded after reflow and its height was about 50 μm. Then we used PDMS (Sylgard 184, Dow Corning, Michigan, USA) to make all the chips. Before the chip fabrication, all molds were exposed to chlorotrimethylsilane (TMCS) vapor for 10 min. Then the two components of PDMS mixed at a ratio of 5 : 1 were poured onto the control channel mold in a Petri dish. PDMS mixture with ratio of 23 : 1 was spin-coated onto the fluidic channel mold at 1000 rpm for 60 s. Both of these two molds were cured in an oven at 80 °C for 30 min. The cured control layer was peeled off from the mold and holes were punched. These two layers were aligned together and baked at 80 °C for 60 min. The two assembled layers were peeled off from the fluidic channel mold and the rest of holes were punched for the access to fluidic channel. Then the chip was placed on a glass slide, which was spin-coated with PDMS (ratio 20 : 1) at 1300 rpm for 60 s and cured at 80 °C for 30 min. Finally, the whole device was put in oven overnight.

Cell culture

The primary human umbilical vein endothelial cells (HUVECs) were isolated from umbilical cord. HUVECs were typically cultured with Medium 199 (M199, Invitrogen) supplemented with 20% heat-inactivated fetal bovine serum (FBS, Invitrogen), 1% penicillin–streptomycin (PS, Invitrogen), 200 mM L-glutamine (Invitrogen), 40 μg ml^{-1} bovine endothelial cell growth factor (bECGF, Roche) and 4000 units heparin (ChangZhou Qianhong Bio-pharma Co., Ltd.). Cells, used for siRNA experiment, were cultured in M199 medium containing 5% FBS, 1% PS and 1% endothelial cell growth supplement (ECGS, Sciencell). (This cocktail for transfection contains less serum to reduce the harm to cells during the 6-hour lipofectamine 2000 (Invitrogen) transfection with non-serum-supplemented medium.) All cells were cultured at 37 °C in a humidified incubator containing 5% CO_2. Cells between passages 2 and 7 were used for all the experiments. When cells became confluent, they were detached by 0.25% trypsin with 0.1% EDTA (Invitrogen), and centrifuged at 1200 rpm for 3 min. Then supernatant was discarded, and cells were re-suspended at a density of 5×10^7 cells per ml. To test the division influence, the cells were treated with Mitomycin C (MMC, Roche) for 2 h before loading on the blank-fill chip. 1 μg ml^{-1} Cytochalasin D (CytoD, Sigma) has been added into the culture medium to inhibit cell division. To facilitate cell migration, we added epidermal growth factor (EGF, invitrogen, 10 ng ml^{-1} or 100 ng ml^{-1}) into the culture medium.

RNA interference

For the siRNA experiments, cells of one 10 cm Petri dish were split into four 25 cm^2 flasks to achieve an appropriate cell density for transfection the next day. Before the lipofectamine transfection, the old medium was replaced with the medium without PS

and FBS. 10 μl lipofectamine 2000 transfection reagent (Invitrogen) was diluted in 500 μl Opti-MEM (Invitrogen), mixed gently and incubated for 5 min at 25 °C. Then 10 μl siRNA (20 μM in DEPC water, Shanghai GenePharma Co., Ltd., China) was diluted in 500 μl Opti-MEM and mixed gently.

The sequences of siRNAs:

HDAC7 siRNAs: 5′-GGACAAGAGCAAGCGAAGUTT-3′, 5′-ACUUCGCUUGCUCUUGUCCTT-3′;

HoxA9 siRNAs: 5′-CGUGCAGCUUCCAGUCCAATT-3′, 5′-UUGGACUGGAAGCUGCACGTT-3′;

AQP-1 siRNAs: 5′-GGGUGGAGAUGAAGCCCAATT-3′, 5′-UUGGGCUUCAUCUCCACCCTT-3′;

NC siRNAs: 5′-UUCUCCGAACGUGUCACGUTT-3′, 5′-ACGUGACACGUUCGGAGAATT-3′.

The diluted siRNA was combined with diluted Lipofectamine 2000, followed by incubation for another 20 min at 25 °C. The whole siRNA-lipofectamine 2000 mixture was added to cells and removed after 6 h incubation in the incubator in order to eliminate the toxicity to cells. Cells were harvested for blank-fill assay, scratch assay, and RT-PCR experiment 24 h after the transfection. Total RNA was extracted with RNAprep pure Cell/Bacteria Kit (Tiangen Biotech (Beijing) Co., Ltd.) and cDNA was synthesized with the PrimeScript Reverse Transcriptase (Takara Biotechnology (Dalian) Co., Ltd.). All of the siRNA knockdown efficiency exceeded 70%, determined by RT-PCR.

Blank-fill assay

Before on-chip cell loading, the entire fluidic channels were coated with fibronectin (200 μg ml^{-1}, Invitrogen), an extracellular matrix protein for 2 h. Then the button valves were actuated and the cells were loaded through the inlets on chip with tygon tubing. When cells became confluent, the button valves were released and phase-contrast images of cells' migration around each blank were recorded by a monochrome CCD camera (2000R, Qimaging, Canada) under a 10X objective of Nikon TE2000-E automated inverted microscope. The blank-fill chip was incubated in a home-made miniature live-cell culture incubator, which was made from plexiglass and fixed on the motorized translational stage (BioPrecision, Ludl Electronic Products Ltd., Hawthorne, NY, USA) of the microscope. This device contained two indium–tin oxide (ITO) glass slides on both the bottom- and top side of the chip. The bottom ITO glass was used to heat the chip and to maintain the temperature at 37 °C. The top ITO glass was used to avoid water condensation on the top of chip. Both of them were controlled through two PID controllers. Chips were partially immersed into water and 5% CO_2 was introduced into the incubator to prevent medium evaporation from the inside of the chip and to ensure the cells on-chip were alive during the whole experiment. The integration among microscope, stage, camera, and chip were automatically controlled by our own script written in MATLAB (Mathworks, Natick, MA, USA), successfully recording time-lapse images with no human input. Every two hours, the old culture medium in the chip microchannels was replaced with fresh one through pneumatic control.

Scratch assay

HUVECs of 50% confluence were transfected with siRNAs, as described above. After 24 h, the cells were transferred to one 6-well plate and incubated for a further 12 h. The medium was aspirated and the "scratch" was created with p200 or p10 pipette tips. Then the cells were washed with D-Hanks twice and the fresh medium without FBS was added to each well to inhibit cell proliferation. At 5 h and 12 h, microphotographs of wound area were taken to determine the speed of cell migration. We took images according to the principle that adjacent images shared some overlap with each other. For each wound, 50 images were taken, covering the whole wound from one end to the other. Image-J was used to manually determine the edge of the wound and the width of each wound was measured at different time points.

Image processing

We developed our own MATLAB script to recognize and calculate blank area from the time-lapse images. In a phase contrast picture, we found that the cell's edge is brighter than its interior (Fig. 1a, step 1), and the variance of the intensity in the region covered by cells is larger than that in the blank region. By setting an appropriate threshold, we could differentiate the blank region from the images. We divided an original image (1600 × 1200 Pixels) into 10 × 10 pixel units and calculated the intensity variance for each of them. If it was larger than the variance threshold we set, we recognized it as a "cell unit", otherwise an "empty unit" (Fig. 1a, step 2). After scanning through all units in the image, a grayscale image was transformed to a binary image, with black representing cell regions, and white representing blank regions (Fig. 1a, step 3). We picked the biggest connected region (Fig. 1a, step 4) and filled all the speckles inside this region as the blank area (Fig. 1a, step 5, 6, in cyan). To speed up the image processing, we cropped 900 × 900 pixel sections from the original time-lapse images, centered on the centroid of the blank region of the first image at time zero, of each single button valve (Fig. 1a, step 7). Our image processing method could accurately locate the blank region at each time point, from the beginning (Fig. 1a, step 8) to the end of the experiment (Fig. 1a, step 9).

Particle Model and Numerical Simulation

To study single-cell migration dynamics, we have constructed a numerical particle model to simulate the whole process of blank-filling. Cells are allowed to move or grow. To move, each cell has nine options, moving in one of the 4 cardinal or 4 ordinal directions and the option of staying still. If there is no collision and the total overlapping areas of all options are smaller than a "crowdedness" parameter, cells may grow (Fig. S2†). Seven parameters, R_{cell}, R_{sense}, P_{random}, P_{grow}, T (Threshold), O (Overall) and R_{max}, are used in our model to simulate cell motion, including movement and growth. For the reason that cell division is rare at the beginning of the blank filling process, we do not incorporate the dividing process in the model. In situation where division is not negligible, cell division can be added to the model.

Each cell is defined as a circular 2-D particle, with a radius of R_{cell} (incompressible internal core). Outside of this core is a sensing part with a width of R_{sense} (compressible external shell).[23] R_{total} is the total radius of a model cell, $R_{total} = R_{cell} + R_{sense}$. R_{max} is the maximum radius the cell may grow to, and the value

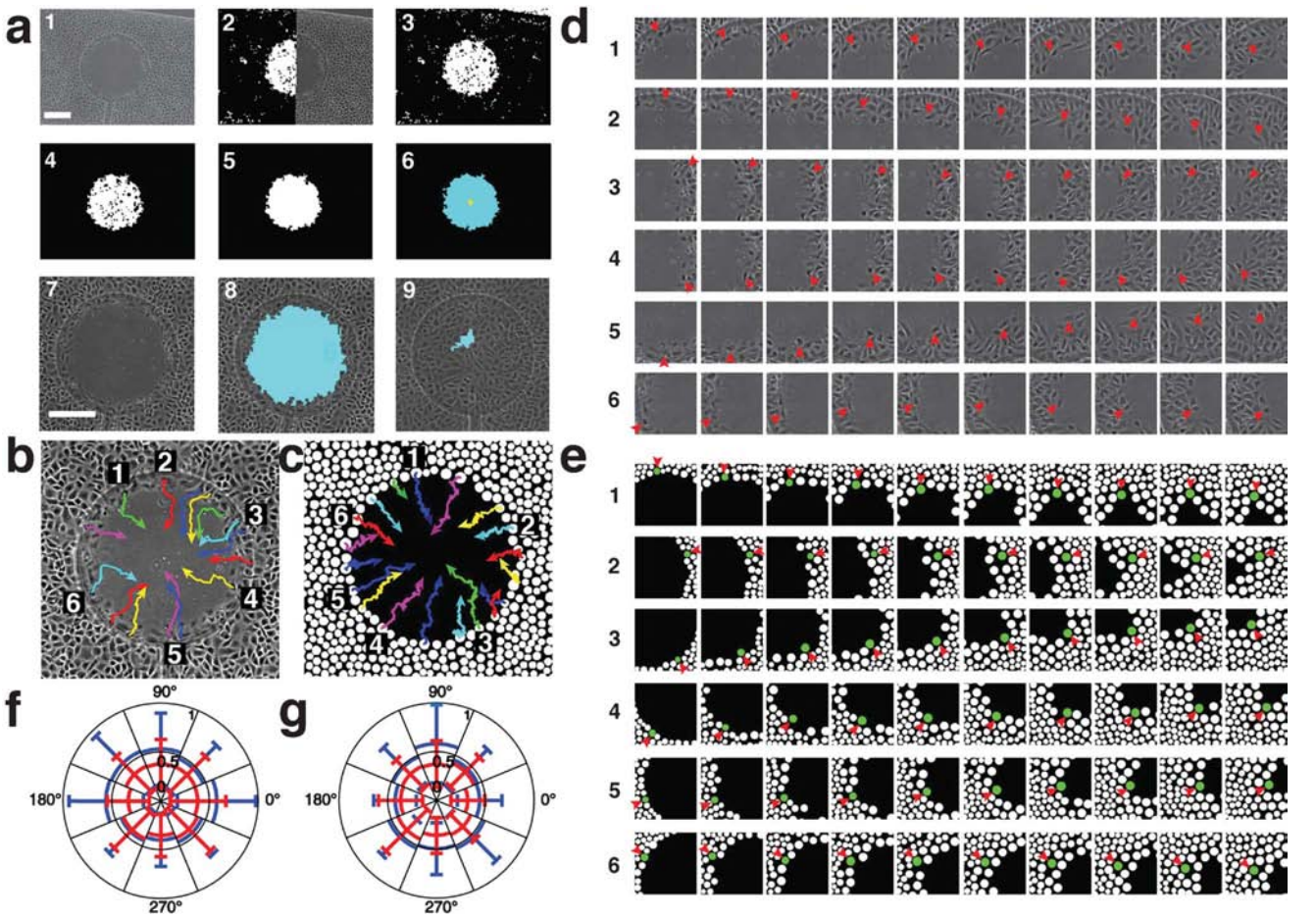

Fig. 1 Blank-fill assay. (a) The image processing procedure. 1) A raw phase contrast microscopic image captured by CCD camera; 2–3) The procedure of scanning the raw image to get the binary image. The areas without cells are marked white and the area with cells are marked black; 4) The biggest connected region kept in the binary image; 5) The biggest connected region with holes filled; 6) The centroid (yellow cross) is determined from the blank (cyan); 7) The cropped image centered on the centroid of the blank region in the first original picture; 8) Non-filled blank region recognized by image processing at the beginning time point; 9) Non-filled blank region recognized by image processing at the ending time point. (Scale bars = 200 μm) (b) Trajectories of single migrating cells clearly show cells' inward movement once the button valve is released (button diameter = 550 μm). (c) Numerically simulated cell trajectories during the migration. (d) Cell migration can be tracked at the single-cell resolution. The tracked cells are also marked in (b). (e) The particle model simulates the single-cell migration. The single particles, marked in (c), are indicated as green spots with arrows. The migration speed of single cells, calculated from the experimental data (f) and from the simulation results (g). Blue and red represented the speed of cells on the edge of the blank or in the area further away from the blank, respectively.

is calculated from the experimental results. P_{random}, P_{grow}, T and O were manually adjusted and kept the same in all simulations. Before simulation, two random numbers between 0 and 1 are generated for each particle, named P_1 and P_2. Before our migration routine, we first calculate the crowdedness for surrounding of each cell. The cell can move in 8 directions ((1,1), (1,0), (1,−1), (0,1), (0,−1), (−1,1), (−1,0), (−1,−1)) or stay still (Fig. S3†). The cell would evaluate these 9 options and check if there is a collision, and then record the overlapped pixels for each evaluation. If no collision occurs and the sum of all overlapped pixels is smaller than the preset parameter O, R_{total} is smaller than R_{max} , and at the same time the random number P_1 is less than P_{grow}, the cell would grow, otherwise the cell would migrate. The parameter P_{grow} controlled the growth rate of each cell and is set to 0.2 for our control group. During growing, R_{total} is increased, while the ratio R_{cell}/R_{sense} keeps the same. The grown cell will evaluate 9 updated options, and then will choose the least overlapped direction to migrate. For migration, the cell first decides whether to walk randomly or migrate with preference, by comparing (1-P_2) with P_{random}. P_{random} represents the probability for a cell to do completely random walk. When P_{random} = 1, all particles will move randomly, while P_{random} = 0 means each individual particle will evaluate its next moving direction and choose a preferred one. In our simulations, P_{random} is set to be 0.2. With this setting, the migration curve is very similar to those with P_{random} = 0, indicating that the cells' motion is not purely random walk.[25] In our simulations, if (1-P_2) is less than P_{random}, the cell would choose to walk randomly. Otherwise, the cell would have to make another decision: if there are options where the overlapping pixels are fewer than T, the cell will choose one of these options randomly; otherwise, the cell would choose the minimal overlapping option. Parameter O is set to control a cell's sensitivity to the crowdedness of its surrounding area. A small O would inhibit the growth of the cell

and make blank areas fill more slowly. Parameter T is used to distinguish one option from the others when several overlapped areas are comparable in multiple options. With a smaller T, the cell would make a smarter choice at each step so the blank area will be occupied faster. The migration curves with different preset parameters are shown in Fig. S4a.†

Even using an identical set of parameters, the simulation is stochastic based on our particle model. To test the robustness of the simulation, we performed fifty repeats of the simulation with the same parameters (Fig. S4b†). We found that the variation was small in the beginning and became gradually larger through the simulation process for the accumulation of randomness. Within the relatively short experimental time required for the blank-fill assay, this simulation is still effective to fit the experimental data.

We set a region of 1950 × 1350 pixel bitmap to match our experiment. Each pixel in the simulation represents one pixel in the experimental images. The cell density for all simulations is obtained from the experiments. A circular area in the center of the region is marked as unreachable to simulate the actuated button valve. The particles are randomly seeded into the accessible area in the region and are spread out evenly. Later, we remove the marked area and the particles start migrating. We calculate the area of the non-filled blank region at each step of the simulation, until the blank is smaller than that of the corresponding experiment. We fit the experimental migration curves by adjusting the parameters, and record the total steps required for each simulation. Then the total time of experiment is divided by the step number, which indicates the time for each simulation step. Since the step size of the simulation is constant, the time for each step reflect the averaging migration speed of single particles.

The numerical simulations were performed in MATLAB. The seeding function and button size calculation were written in MATLAB, while cell migration function was written in C, running in parallel through CUDA (nVIDIA, Santa Clara, CA, US) on a GT200b GPU. Each cell was assigned to a thread on the GPU.

To compare with our blank-fill assay, we also simulated the wound healing process in the conventional scratch assay (Fig. S5†). The width of the scratch, representing the wound, was set to be equal to the diameter of our button valve (550 μm). We simulated the wound healing process using the parameters that have been used in our blank-fill assay simulation. We simulated two different cases, one with the same cell density and size as our chip experiment, another with bigger cell and lower density, as what we measured in the scratch assay.

Results and discussion

Blank-fill chip working principle

It is critical to resolve the subtle difference of cell's migration speed under different treatments, and to verify or score the migration regulatory genes in living cells. However, conventional scratch assay often produce data with less-than-desired accuracy. To evaluate the epigenetic regulation of HUVECs' migration, we have developed an integrated microfluidic chip called the "blank-fill chip" (Fig. 2), which is inspired by "MITOMI chips".[22] The original design has been used for capturing the intermolecular interactions with large dynamic range while our modified version is aimed at creating uniform and highly parallel blank regions among the cell monolayer. These blanks, generated through modified pneumatic "button valves", are used to emulate wounds (Fig. 2a).

Unlike the common pneumatic control valves in microfluidic chips,[20,21] the size of the button valve is slightly smaller than the flow channels. Under zero external pressure, a button valve remains flat (Fig. 2c,d). When pressure is applied, the valve is deflected downwards to block part of the bottom surface of the flow channel (Fig. 2e,f, and Movie 1†), creating a "blank" area, which the liquid inside the flow channel cannot access, thus ensuring that cells cannot enter during seeding. After the cells fully attach the surface and grow to confluence, the button valves can then be released to allow the cells to migrate into the blank (Fig. 2a), and an automated optical microscope records time-lapse images of cell motion.

Scratch assay

Conventionally, scratch assay is widely used to measure the cells' motility by calculating the speed of gap closing within a cell monolayer. However, the edge of the gap, usually generated by scratching the cell monolayer with a pipette tip, is rough (Fig. 2g). This makes the gap measurement and data analysis unreliable, subjective, and often irreproducible. The width of the gap is controlled by the physical size and shape of the pipette tip, and the force applied to make the scratch. The typical width in previous reports varies from a few hundred of micrometers to a few millimetres. Recently researchers start studying migration by creating a blank among cell monolayer and observing the cell moving into the blank. The blanks could be created by releasing self-assembly monolayers,[16] by polymeric phase-transition,[11] or by mechanically blocking certain areas in the well plates.[12] These approaches have generated migration data with higher accuracy than scratch assays. However, some of these methods require surface pretreatment or patterning[16] which may conflict with certain cell culture conditions, and some still require long time to observe the migration and these long time experiment, conflating the effect of migration and proliferation.[11] We have set our button's diameter to be 550 μm to create multiple identical wounds for each experimental condition. The size of the button fits HUVECs' averaging migration speed, allowing the whole blank-filling process to be finished in a few hours.

Typically, a scratch assay uses the percentage of the gap-width reduction at certain time points to represent the migration speed. Although the wounding of the scratch assay is intuitively simple and requires minimal setup, damages to the cells at the edge of the wound complicate the data analysis. Furthermore, as migration proceeds, the edge of the scratch roughens and becomes irregular, making it even more difficult to track the moving front (Fig. S1 and Movie 2†).

We tested the epigenetic regulation of HUVECs by knocking down HDAC7 through RNA interference, and observed the change of migration speed using conventional scratch assays. We also knocked down two other genes, Homeobox A9 (HoxA9) and aquaporin-1 (AQP-1), as comparisons because the silencing of these two genes has been reported to negatively regulate HUVEC motility as well.[24,25] It has been reported that HDAC7

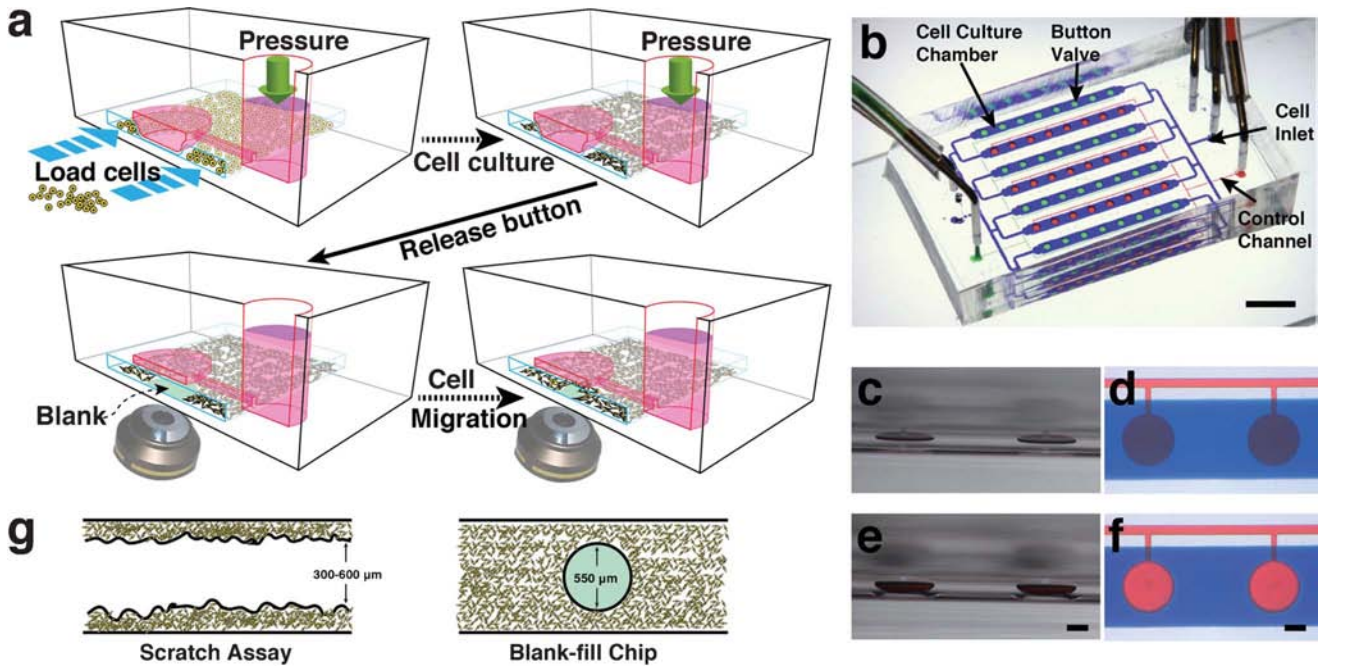

Fig. 2 The blank-fill chip. (a) The work-flow of the assay (items not to scale). Step 1: Suspended cells are loaded into the culture-channels while the button valves are pressurized. When the buttons are actuated, the lower membrane of the button valve will expand and then partially block the surface of the culture channels. Step 2: The cells then adhered to the surface and grow inside of the micro-channels to confluence. Step 3: When the button valve is released the blank is created among the cell layer. Step 4: The cells migrate into the blank after the release of the button valves. We capture the time-lapse images of the migration process for each button valve and use these images to calculate the migration speed. (b) An actual blank-fill chip (scale bar 5 mm). This chip has 64 button valves that can handle 8 groups of experiments with 8 repeats in parallel. To indicate the multi-layer architecture of the chip, the button valves are filled with green and red dyes, and the cell-culture channels are filled with blue dye. (c) and (d) are top-view and side-view close-ups of the valves without pressurization; (e) and (f) are the cases of the valves actuated under the hydraulic pressure (scale bar = 200 μm). (g) Schematic illustration of wounds generated by scratch-assay and the blank-fill assay. The blank generated by pneumatic button valves is more controllable and uniform.

controls PDGF-B expression and thus activates PDGFR/PI3K/Akt pathway,[8] and HoxA9 gene, which is directly related to HDAC7, encodes a transcription factor, which regulates EphB4 receptor expression and then also activates PI3K/Akt/MMP pathway.[24] Aquaporin-1, which encodes a water channel protein that may facilitate the rapid turnover of cell membrane protrusions at the leading edge,[25] has not shown any direct relationship with HDAC7. We transfected specific siRNAs to down-regulate the expression of those genes by >70% and recorded those cells' migration.

As expected, the edge of the scratch is not straight and during the migration the edges become even more irregular (Fig. 3a). We followed the conventional way to manually analyze each set of experiments at 50 different spots along the length of the gap. The result was highly subjective and depended critically on the end point of each experiment (Fig. S1†). This result is marked in Fig. 3c as solid circles. We have developed our image-processing algorithm to differentiate the cell edges and the wound gap, and to obtain a statistical assessment of the gap width distribution. We found that the noisiness of the scratch generation and the inherent irreproducibility of the scratch assay led to quantitatively unreliable measurements. The histograms in Fig. 3b show the gap width distribution along the scratched wounds at 0 h and 5 h. The dispersion of the gap width made it difficult to accurately determine the migration speed. If we take the mean width of the gap to calculate the migration (presented as bars in Fig. 3c), and compared with the manually obtained results, not only the final values of the migration speed are different by using different methods, the relative speed difference between samples is also not consistent.

Single-cell migration analysis

Phase contrast microscopic images of each blank are taken every 6 min and stored. The cell-covered area and blank of each image are separated and calculated with our own image-processing program (Fig. 1a) to obtain the area *vs.* time migration curves and to calculate motility. Dynamically observed under the microscope, we can track the motion of every cell in the field of view. We illustrate a few trajectories of cell migration in Fig. 1b,d. While each cell's initial direction appears random, as a population, the cells migrate inwards to fill the blank (Movie 3†).

To describe the migration dynamics more quantitatively, we model the microscopic process with a "particle" model (Fig. S2†). Each cell is regarded as a solid particle with an incompressible hard *core* and a partially compressible soft shell.[23] A cell's shell is allowed to overlap with another shell or core, while two cores cannot collide. We found that this model is a simple but effective way to simulate single-cell motion. We picked a few single cells around the blank region and traced their trajectories during blank-fill (Fig. 1c,e). The cells around the edge of the blank have longer travelling paths and larger

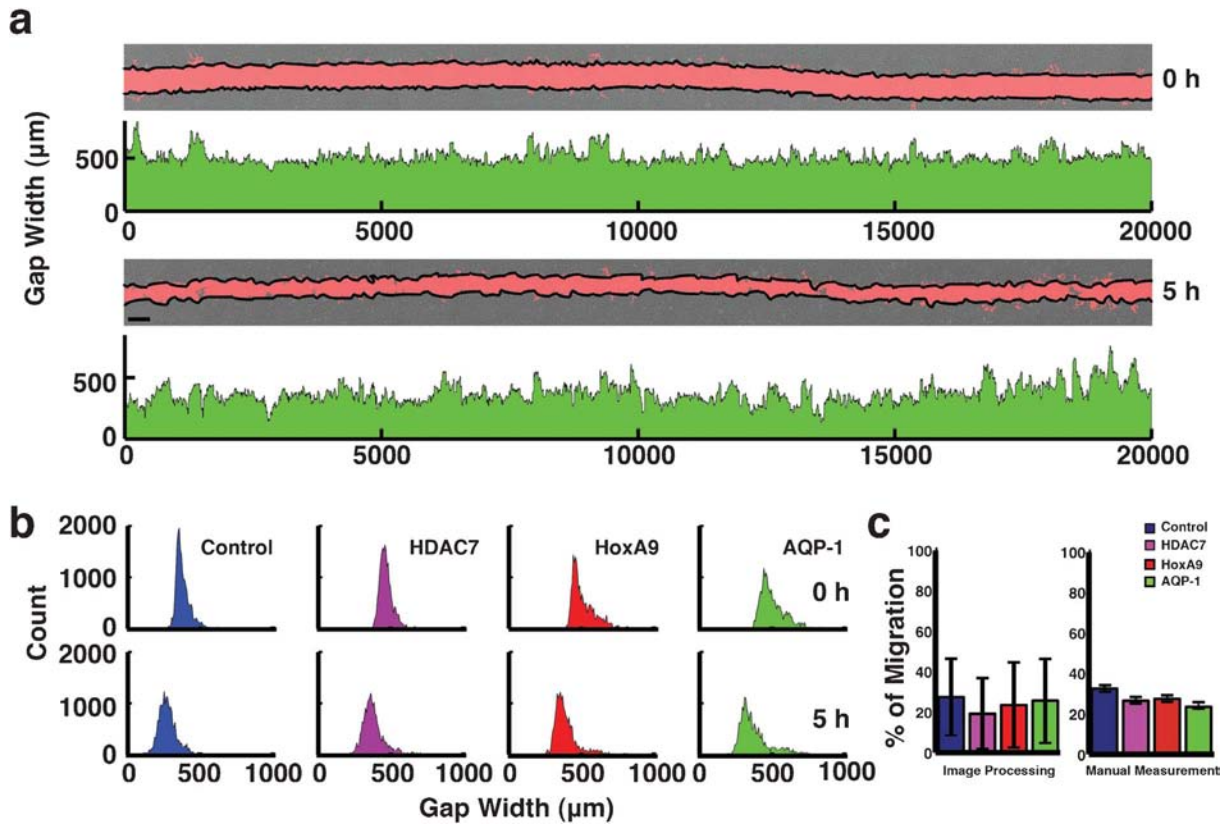

Fig. 3 The scratch assay of HUVEC migration. (a) Each of the overall pictures of the whole scratch around 15 mm is stitched from 50 microscopic images. The red-marked area is the scratch determined by automatic image processing while the black lines are drawn manually to indicate the frontiers of cells. The gap width is reduced through cell migration. (b) RNAi of HDAC7, HoxA9, and AQP-1 with conventional scratch assay. Knocking down of these three genes effectively slows down the migration speed of HUVECs. The distribution of gap width through the whole scratch is dispersive, causing difficulty to obtain the frontier of the cells accurately. (c) Motility calculated from conventional scratch assays. Migration can be quantified using the percentage of the reduction of the scratch gap. Knocking down HDAC7, HoxA9 or AQP-1 will slow down the migration speed, which is confirmed both by manual measurement and automatic image processing. However, two methods give inconsistent motility measurement.

displacement than the cells that stay further away from the blank. Through frame-by-frame cell location tracking, we can calculate the cell moving speed and direction at the single-cell level. We randomly chose 40 cells for analysis, 32 from the edge of the blank and 8 from the area further away from the blank. The statistics of single-cell motion are summarized in Fig. 1f,g, showing that when we consider each group of cells as a whole, the single-step motions are omnidirectional and the cells sitting at the blank edge move much faster than the others. This result indicates that the cells around the wound are the major players of migration and lead the wound healing process, and analysis of their motion will faithfully unveil the cell autonomous mobility. Although this single-cell resolution method is effective to obtain the individual cell's migration speed, a simpler expression of the collective migration is still valuable to quantitatively evaluate the wound healing process.

Blank-fill assay of HUVEC migration

A few hypotheses have been proposed to explain the migration behaviour caused by different shapes of the cell patterns and the edge effects.[26,27] To verify whether different shapes of the blank trigger different migration phenotypes along the filling process, we designed a chip with three different shapes of button valves. We did not observe any obvious intercellular mechanical shear effect, which might occur when the cells were too crowded,[28] affecting their autonomous motion. We found that although the initial areas are the same, circular blanks filled more slowly than the other shapes (Fig. 4a). We speculate that this is because the migration process is controlled by the perimeter of the blank region, namely, the population of cells on the edge of the blank region. Therefore, a simple dynamical process can be used to describe migration in the blank-fill chip. The average migration process is controlled by the population of cells on the perimeter of the blank region and can thus be modeled as:

$$\frac{dA}{dt} = ka_0 A^{\frac{1}{2}} \quad (1)$$

where A is the blank area, a_0 is a normalization coefficient, and k is the non-dimensional migration speed. By fitting the experimental data to our particle model and to eqn (1), we extract a single parameter (k) to represent the cell's motility, providing an objective and highly quantitative assessment. The initial-shape-dependent k value indicates that identical blanks are necessary to perform the reliable comparison in parallel. With our blank-fill device, the blanks are created with great accuracy. Moreover, this miniature device provides a unique solution to separate cell

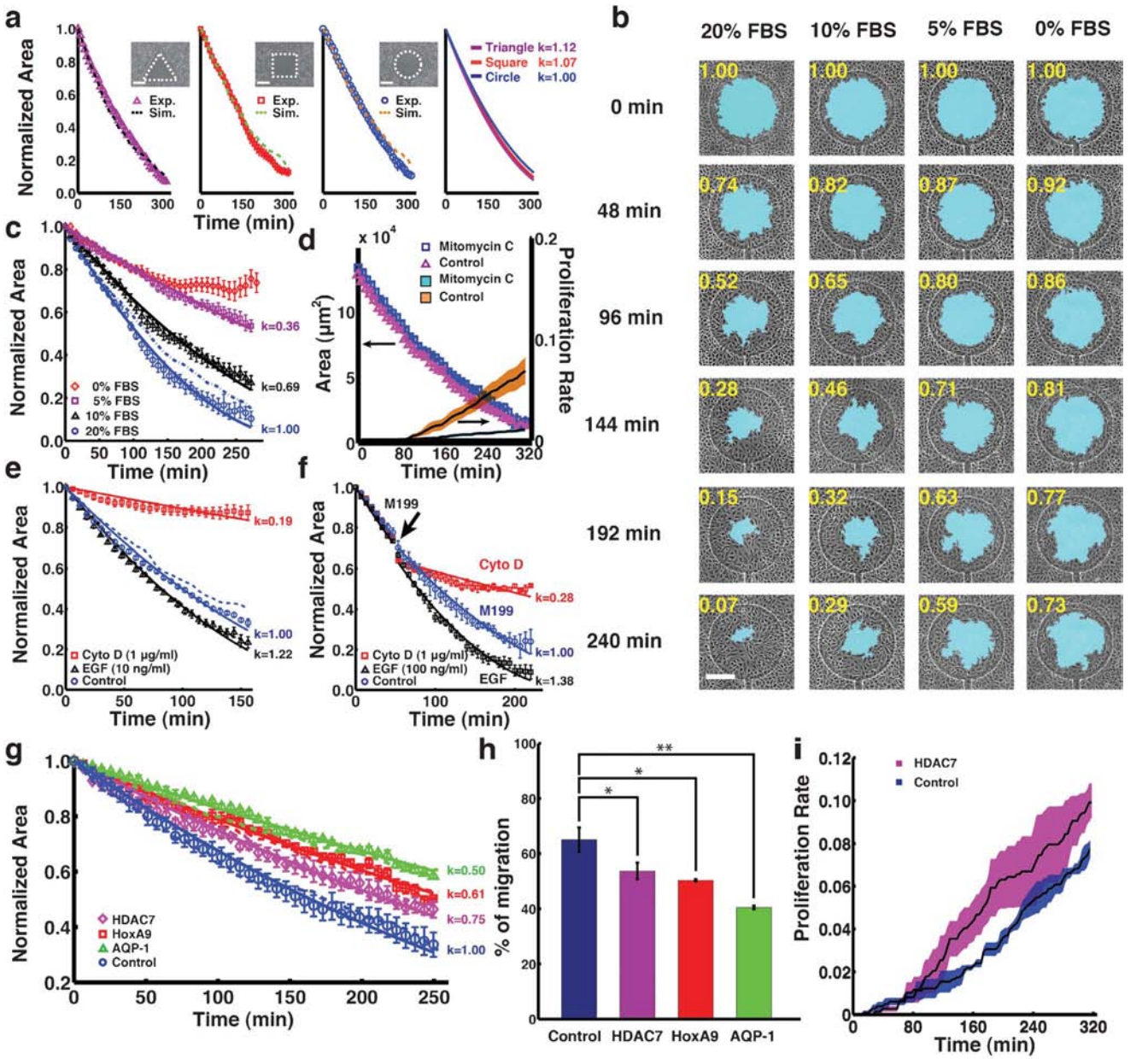

Fig. 4 Migration curves are plotted through image analysis of blank-filling process. The remaining area of the blank is calculated by automatically analyzing each time-lapse image of each button valve. (a) The shape of the button slightly affects the migration curve fitting and the k value reflects the shape dependence. We use both numerical simulation and eqn (1) to fit the experimental data. (b) Reducing the concentration of FBS in culture medium slows down the HUVECs' migration speed (scale bar 200 μm). The relative ratio of the blank area during migration is noted in each panel. (c) The experimental migration curves are plotted as open symbols with error bars representing variation from multiple replicates within a single culture channel. The solid and dash lines are fitting results by using eqn (1) and numerical simulations, respectively. (d) Migration curves of HUVECs with and without proliferation inhibitor Mitomycin C. The open symbols represent the calculated area of blank at different time points during the migration. The solid lines are counted proliferation rate and for each condition, the variation from 8 groups of experiment is represented by a color blanket. (e) The migration curves show that EGF facilitates migration while CytoD inhibits cell motion. (f) With microfluidic control, the culture condition can be swiftly changed *in situ* and cell migration swiftly responds to the microenvironmental changes. (g) Fitting the on-chip migration curves by eqn (1) gives the non-dimensional migration speed k of each curve. (h) Taking the area reduction of the blank at $t = 4$ h as the indicator, we can obtain quantitatively reproducible results of migration with higher accuracy. (i) The proliferation rate of HUVECs with HDAC7 RNAi.

migration and proliferation, both of which contribute to the wound closing process.

In conventional migration assays, which typically last more than 12 h, it is common to inhibit proliferation by decreasing serum concentration[10] or by applying drugs, such as Mitomycin C (MMC).[29] Both practices put cells into unnatural conditions, which could lead to misleading assessments of cell motility. Serum is crucial for cell sustainment and proliferation. We compare four experiments with different concentrations of fetal bovine serum (FBS) on a single chip. Fig. 4b shows time-lapse

images of the blank (in cyan). Fig. 4c shows that both numerical simulation and eqn (1) fit well the experimental data and that the lower the serum concentration, the slower the cells migrate. These results demonstrate that the low levels of serum in conventional assays might lead to incorrect assessments of the migration speed. By using circular button valves with diameters of 550 μm, which are small enough to observe the cell migration within 5 h, we avoid the need to suppress proliferation and can, for the first time, investigate quantitatively the effects of MMC (Fig. 4d, Movie 5†) and serum concentrations on cell migration. Two experiments, with and without proliferation inhibitor Mitomycin C in the culture medium, are performed in parallel. The division events inside the field of view are counted in both cases. Cell division is rare at the beginning of the blank filling process, only 8% for the control group, indicating that division is negligible during the early period of experiment.

Our blank-fill chip is highly controllable and flexible. It has been reported that epidermal growth factor (EGF) can stimulate HUVEC migration,[30] while Cytochalasin D (CD), which binds to actin,[31] directly inhibits cell migration. Through the microfluidic control of our blank-fill chips, stimuli can be applied *in situ* accurately, precisely, and dynamically. We found that compared with normal culture medium, CD (1 μg ml^{-1}) significantly hindered cell migration, while EGF (10 ng ml^{-1}) boosted motility (Fig. 4e). The solution in our blank-fill chip can be changed rapidly through the use of integrated valves. Fig. 4f shows that after a prompt change in the microenvironment at 50 min into the experiment, the migration curves immediately separated. When EGF concentration (100 ng ml^{-1}) was further increased, cells migrated even faster (k = 1.38, Fig. 4f) than what we had observed in the previous experiment (k = 1.22 for 10 ng ml^{-1} EGF, Fig. 4e).

The capability of differentiating subtle changes in migration speeds makes blank-fill chips ideal to study epigenetic regulatory on cell motility. The result obtained from this chip-based assay is shown in Fig. 4g. Similar to the result from conventional approach, all three RNAi experiments on-chip lead to the decrease of migration speed, while the global view of the whole dynamic process provides more accurate assessment through analyzing the entire migration curves. The speed of migration under each condition can be automatically extracted precisely and reliably. Both numerical simulation and eqn (1) have been applied to obtain the motility of cells and the comparison of these two approaches is listed in Table 1. The motility fitted through numerical simulation is the migration speed of every single cell, calculated at each time step, while the motility fitted through the analytical equation represents the collective migration speed of a group of cells. We found that the results derived from these two methods well match each other, except that the single-cell motility simulation using the particle model does not depend on the initial shape. With the design of identical circular shape blanks, the fitted k values can also depict the average migration speed of individual cells.

We also implement the end-point analysis for our data obtained on-chip (Fig. 4h) to evaluate the performance of our method through comparison with previous result from the experiment in well plates (Fig. 3c). There are two major improvements. Firstly, the determination of the migration speed is more quantitative with much smaller errors. Secondly, the relative effectiveness of the speed reduction has been estimated with higher confidence level. Epigenetic regulation of migration through HDAC7 silencing is not as direct as the down-stream interference such as HoxA9 or AQP-1. We also found that the reduction of migration speed through HDAC7 knock down is not as affect as silencing the HoxA9 or AQP-1. This difference was not able to be unveiled using scratch-assay because the data is not completely objective. The cell division, which may also be altered through RNAi during the long-term healing process, may also slightly affect the result. The accurate control and precise observation at the single-cell level are able to provide new insight of the epigenetic regulation to cell migration. With our blank-fill device, we also check the proliferation rate of HUVECs with HDAC7 knocked down. Although previous studies have suggested that HDAC7 RNAi will not affect cell growth,[8] we clearly observe the increase of proliferation rate compared to the control group (Fig. 4i).

Table 1 The motility calculated from numerical and analytical methods

		Numerical	Analytical
Button shape	Circle*	1.00	1.00
	Square	0.96	1.07
	Triangle	0.96	1.12
Stimulation	Control*	1.00	1.00
	CytoD	—	0.19
	EGF	1.70	1.22
FBS concentration	20%*	1.00	1.00
	10%	0.81	0.69
	5%	0.44	0.36
RNAi	Control*	1.00	1.00
	HDAC7	0.86	0.75
	HoxA9	0.67	0.61
	AQP-1	0.58	0.50

* Experimental group used for normalization.

Conclusions

We quantitatively investigate the epigenetic regulation of HUVECs through a precisely controllable microfluidic blank-fill chip. This method offers high-throughput and reproducible way to observe cells' collective and individual migration with single-cell resolution. We develop a particle model to simulate the single-cell migration behaviour, as well as a simple analytical expression to fit the migration curves and extract the motility. Blank-fill chips can generate identical wounds without harms to the cells. Besides the advantages of little consumption and robust control, this method shortens the experimental time, thus reducing the effects of division, and represents significant improvements over conventional scratch assay and other wound-healing assays. RNAi of HDAC7 slows down the HUVEC migration, but slightly facilitates the division. Compared to conventional scratch-assay, our quantitative assessment is of much less error, clearly differentiating the strength of the reduction of migration speed between different RNAi targets. We believe this method can also be seamlessly applied to many other cells other than HUVECs. Excepting the limitation that the circular shaped lesion may not reflect a natural wound, this highly quantitative method, based on automatic operation through precisely controllable microfluidic devices and model-based data analysis, is parallel and highly

scalable, and thus holds great potential to be used as large-scale migration assays in the laboratory and for drug and functional gene screenings.

Acknowledgements

The authors thank Haidian Maternal and Children's Health Hospital for providing HUVECs, and Drs. Fuchou Tang, Wensheng Wei, Li Yu, Jianzhong Xi, and Yuan Yao for fruitful discussion. Funding for this work was kindly provided by the National Key Basic Research Program of China (973) (2011CB809105, 2011CB809106, 2007CB714502), the National Natural Science Foundation of China (90 913 011, 20 905 004), the Ministry of Education of China (NCET-08-0016), and the Fok Ying Tung Education Foundation.

References

1 A. J. Ridley, M. A. Schwartz, K. Burridge, R. A. Firtel, M. H. Ginsberg, G. Borisy, J. T. Parsons and A. R. Horwitz, *Science*, 2003, **302**, 1704–1709.
2 P. Friedl and D. Gilmour, *Nat. Rev. Mol. Cell Biol.*, 2009, **10**, 445–457.
3 J. Yuasa-Kawada, M. Kinoshita-Kawada, Y. Rao and J. Y. Wu, *Proc. Natl. Acad. Sci. U. S. A.*, 2009, **106**, 14530–14535.
4 C. Decaestecker, O. Debeir, P. Van Ham and R. Kiss, *Med. Res. Rev.*, 2007, **27**, 149–176.
5 K. J. Simpson, L. M. Selfors, J. Bui, A. Reynolds, D. Leake, A. Khvorova and J. S. Brugge, *Nat. Cell Biol.*, 2008, **10**, 1027–1038.
6 F. Rahnama, F. Shafiei, P. D. Gluckman, M. D. Mitchell and P. E. Lobie, *Endocrinology*, 2006, **147**, 5275–5283.
7 A. J. de Ruijter, A. H. van Gennip, H. N. Caron, S. Kemp and A. B. van Kuilenburg, *Biochem. J.*, 2003, **370**, 737–749.
8 D. Mottet, A. Bellahcene, S. Pirotte, D. Waltregny, C. Deroanne, V. Lamour, R. Lidereau and V. Castronovo, *Circ. Res.*, 2007, **101**, 1237–1246.
9 S. Wang, X. Li, M. Parra, E. Verdin, R. Bassel-Duby and E. N. Olson, *Proc. Natl. Acad. Sci. U. S. A.*, 2008, **105**, 7738–7743.
10 C. C. Liang, A. Y. Park and J. L. Guan, *Nat. Protoc.*, 2007, **2**, 329–333.
11 H. Tavana, K. Kaylan, T. Bersano-Begley, K. E. Luker, G. D. Luker and S. Takayama, *Adv. Funct. Mater.*, 2011, **21**, 2920–2926.
12 W. Gough, K. I. Hulkower, R. Lynch, P. McGlynn, M. Uhlik, L. Yan and J. A. Lee, *J. Biomol. Screening*, 2011, **16**, 155–163.
13 C. R. Keese, J. Wegener, S. R. Walker and I. Giaever, *Proc. Natl. Acad. Sci. U. S. A.*, 2004, **101**, 1554–1559.
14 F. Q. Nie, M. Yamada, J. Kobayashi, M. Yamato, A. Kikuchi and T. Okano, *Biomaterials*, 2007, **28**, 4017–4022.
15 M. Poujade, E. Grasland-Mongrain, A. Hertzog, J. Jouanneau, P. Chavrier, B. Ladoux, A. Buguin and P. Silberzan, *Proc. Natl. Acad. Sci. U. S. A.*, 2007, **104**, 15988–15993.
16 L. Wang, J. Zhu, C. Deng, W. L. Xing and J. Cheng, *Lab Chip*, 2008, **8**, 872–878.
17 M. R. Doran, R. J. Mills, A. J. Parker, K. A. Landman and J. J. Cooper-White, *Lab Chip*, 2009, **9**, 2364–2369.
18 E. E. Hui and S. N. Bhatia, *Proc. Natl. Acad. Sci. U. S. A.*, 2007, **104**, 5722–5726.
19 H. S. Zhang, Y. Hao, J. Y. Yang, Y. Zhou, J. Li, S. Y. Yin, C. H. Sun, M. Ma, Y. Y. Huang and J. J. Xi, *Nat. Commun.*, 2011, **2**, 554.
20 M. A. Unger, H. P. Chou, T. Thorsen, A. Scherer and S. R. Quake, *Science*, 2000, **288**, 113–116.
21 T. Thorsen, S. J. Maerkl and S. R. Quake, *Science*, 2002, **298**, 580–584.
22 S. J. Maerkl and S. R. Quake, *Science*, 2007, **315**, 233–237.
23 M. Bindschadler and J. L. McGrath, *J. Cell Sci.*, 2007, **120**, 876–884.
24 T. Bruhl, C. Urbich, D. Aicher, A. Acker-Palmer, A. M. Zeiher and S. Dimmeler, *Circ. Res.*, 2004, **94**, 743–751.
25 S. Saadoun, M. C. Papadopoulos, M. Hara-Chikuma and A. S. Verkman, *Nature*, 2005, **434**, 786–792.
26 D. A. Lauffenburger and A. F. Horwitz, *Cell*, 1996, **84**, 359–369.
27 X. Jiang, D. A. Bruzewicz, A. P. Wong, M. Piel and G. M. Whitesides, *Proc. Natl. Acad. Sci. U. S. A.*, 2005, **102**, 975–978.
28 P. A. Janmey and C. A. McCulloch, *Annu. Rev. Biomed. Eng.*, 2007, **9**, 1–34.
29 A. Besson, M. Gurian-West, A. Schmidt, A. Hall and J. M. Roberts, *Genes Dev.*, 2004, **18**, 862–876.
30 M. Nakamura and T. Nishida, *Cornea*, 1999, **18**, 452–458.
31 J. A. Cooper, *J. Cell Biol.*, 1987, **105**, 1473–1478.

Electronic Supplementary Material (ESI) for Lab on a Chip

Supporting Information

Live cell imaging analysis of the epigenetic regulation of the human endothelial cell migration at single cell resolution

Chunhong Zheng,[a,b,1] Zhilong Yu,[a,b,1] Ying Zhou,[a,b,1] Louis Tao,[c] Yuhong Pang,[a,b] Tao Chen,[a,b] Xiannian Zhang,[a,b] Haiwei Qiu,[a,2] Hongwei Zhou,[a,b] Zitian Chen,[b,d] and Yanyi Huang[a,b,d,2]

[a] College of Engineering, Peking University, Beijing 100871, China.
[b] Biodynamic Optical Imaging Center (BIOPIC), Peking University, Beijing 100871, China.
[c] Center for Bioinformatics, National Laboratory of Protein Engineering and Plant Genetics Engineering, College of Life Sciences, Peking University, Beijing 100871, China.
[d] College of Chemistry and Molecular Engineering, Peking University, Beijing 100871, China.

[1] These authors contributed equally to this work.
[2] To whom correspondence should be addressed. E-mail: yanyi@pku.edu.cn.

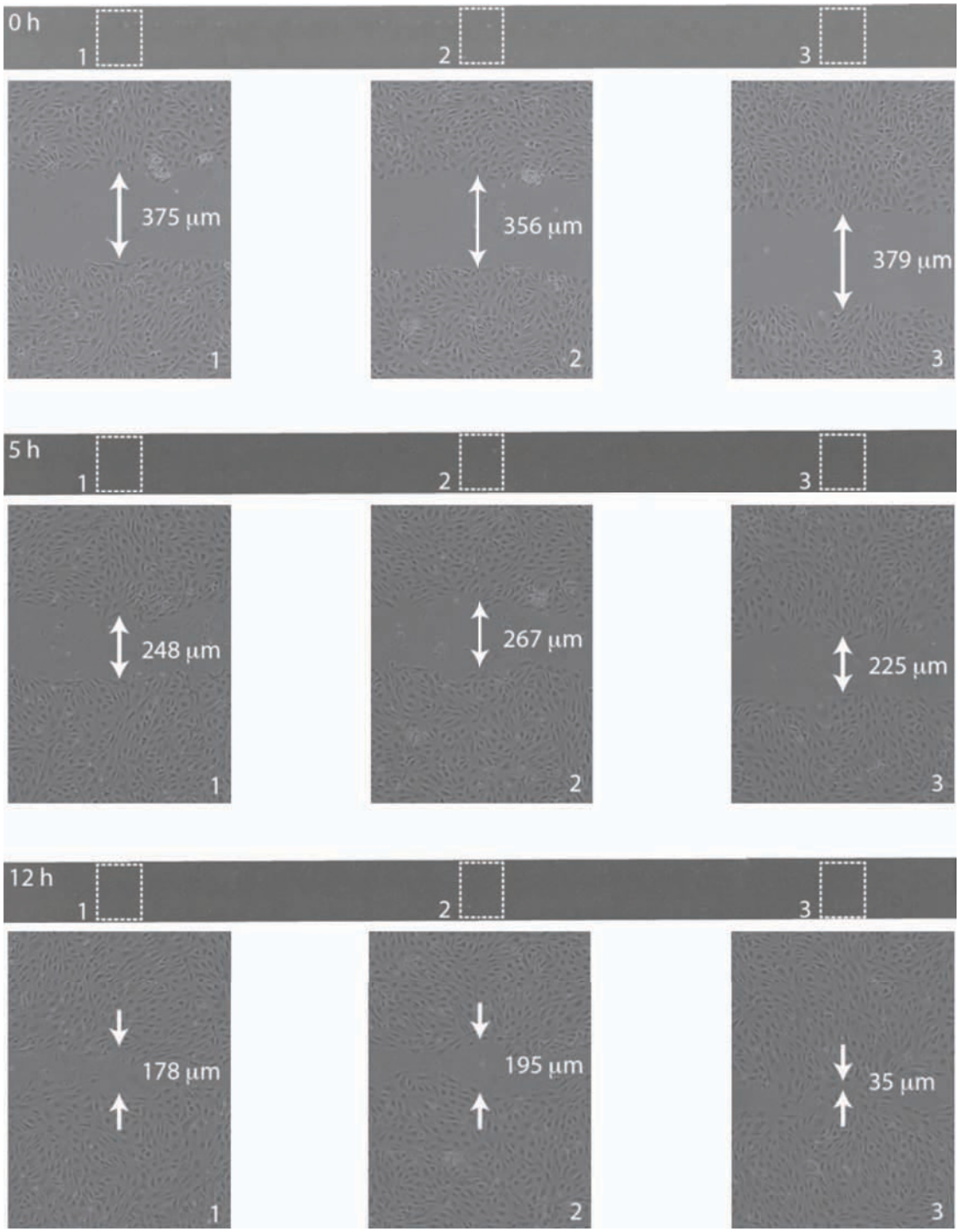

Fig. S1. We show a typical scratch on a layer of HUVECs and the "healing" process with time, using the conventional scratch assay. In the experiment we need to pick 50 spots along the scratch and then measure the remaining width of the gap. We show zoomed pictures of three spots at 0 h, 5 h, and 12 h after the scratch generation, demonstrating the dispersive distribution of the gap width along cell migration.

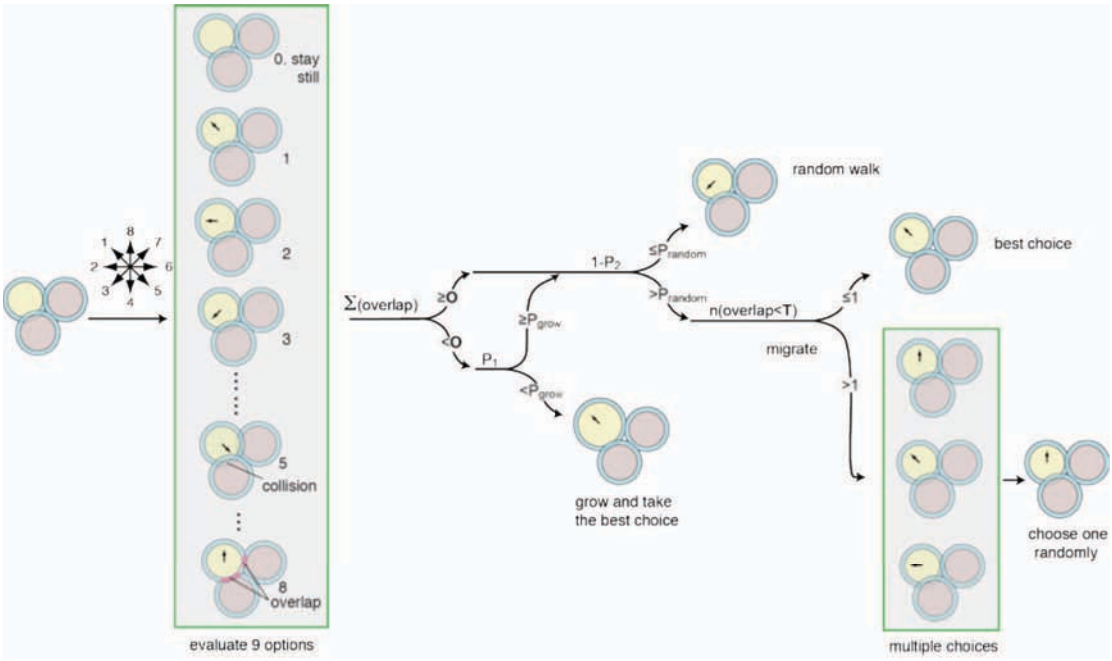

Fig. S2. A numerical method has been developed to simulate the cell motion. We evaluate 9 different moving options for each individual cell at each step, and then choose one option to avoid collision. For each direction, the cells will have certain possibility to grow when migrating, as we have observed in the experiments.

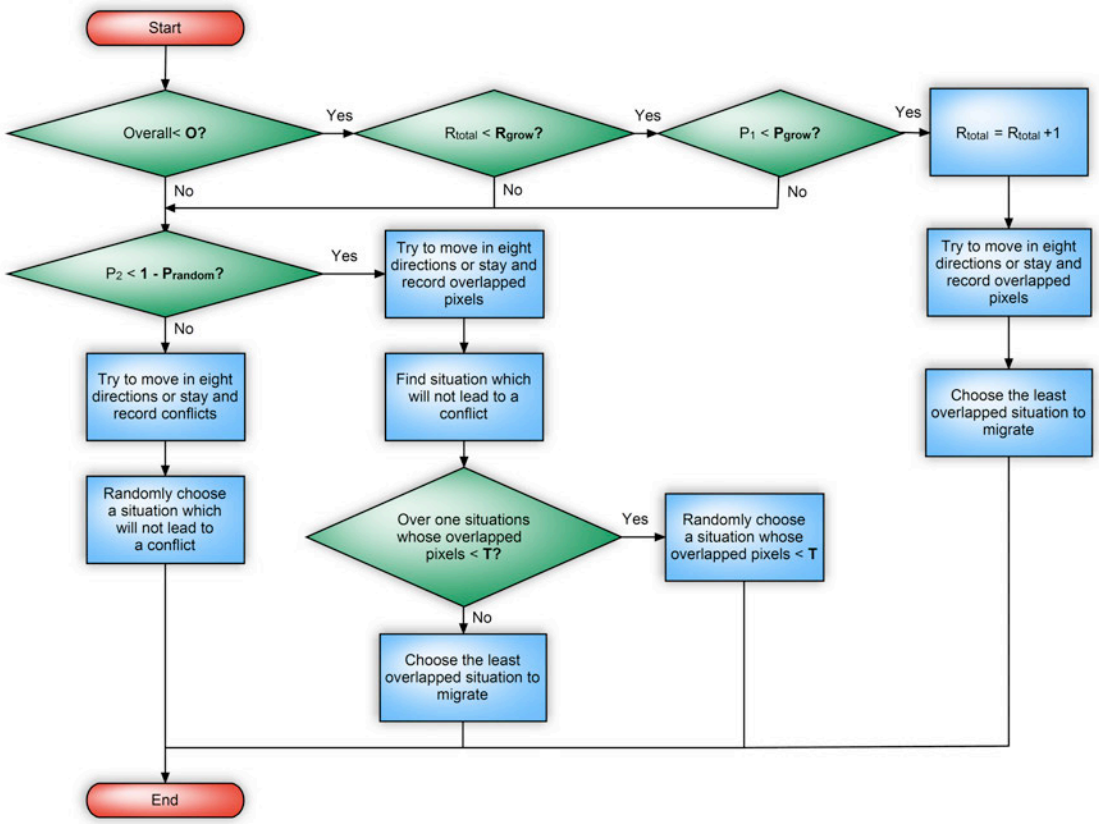

Fig. S3. The flow chart of numerical simulation. The detailed description is in the Supplementary Methods.

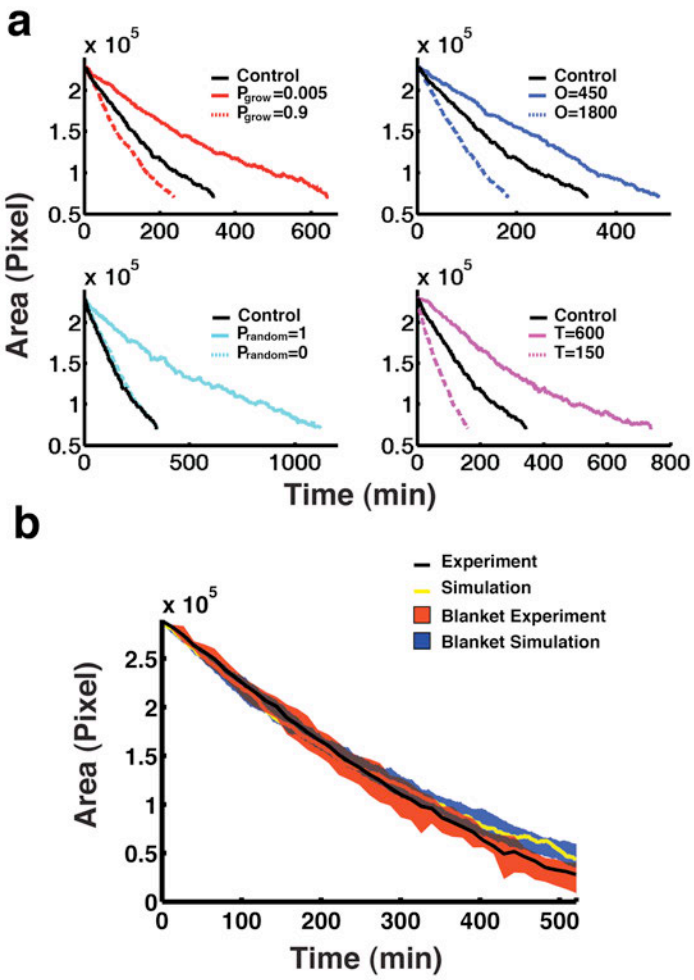

Fig. S4. Simulation of blank-filling through the particle model. (A) The effect of different parameters for simulation. All black lines are generated from simulations with the same set of parameters (P_{grow} = 0.8, P_{random} = 0.2, O = 900, T = 300), labeled as “control” group. Color lines (solid and dashed) represent simulation results with different parameters. For each subgroup, one parameter is changed while keeping the other three the same of the control group. (B) The stochastic effect of numerical simulation is demonstrated by fifty independent runs using same parameters. The blue blanket represents the result of fifty simulation runs and the red blanket shows the experimental result.

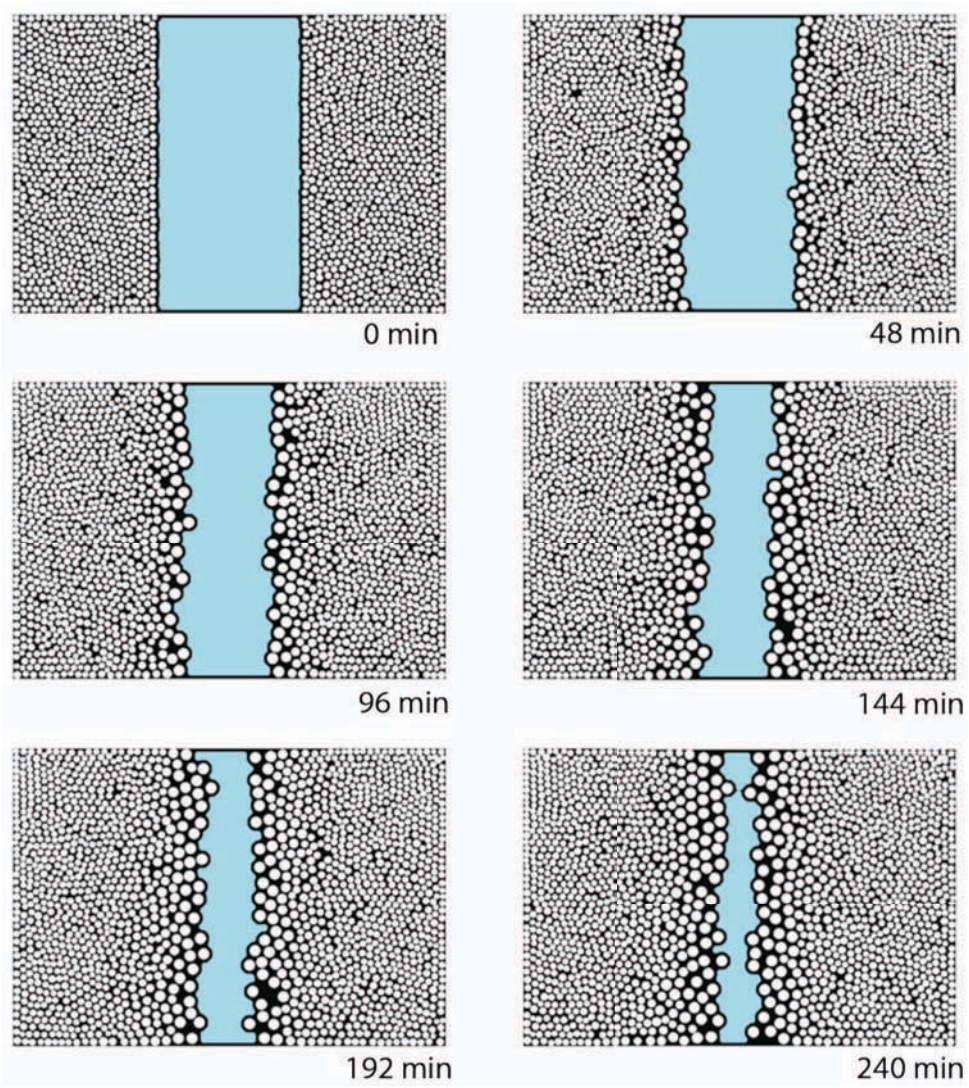

Fig. S5. Simulation of the scratch assay (550 μm gap) using particle model, showing that the wound gap (cyan) becomes irregular during the migration.

Code #1 (

SI Movie 1.

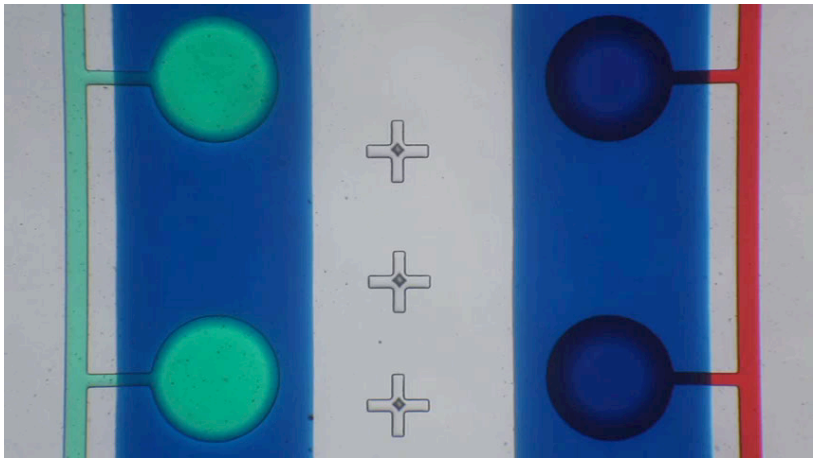

The button valves are actuated by pneumatic pressure. This movie shows two individually controlled groups of button valves driven sequentially. The buttons are filled with red or green dyes while the culture channels are filled with blue dye. During the actuation, the liquid inside the culture channel but beneath the buttons will be pushed away; hence the buttons will turn into red or green.

SI Movie 2.

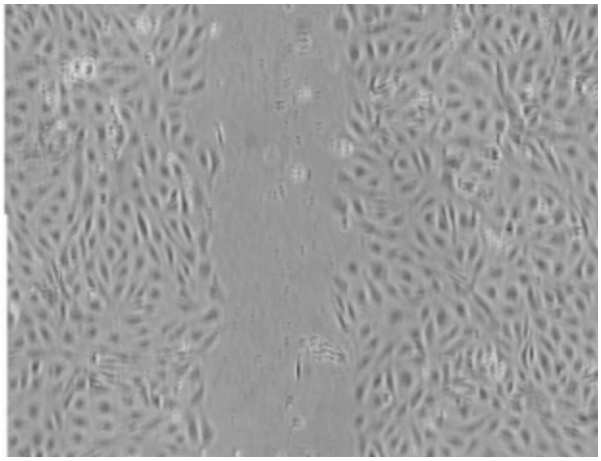

The microscopic view of a wound generated by scratch assay at different time points during the experiments. With cell migration, the irregularity of the wound edge is creased, causing difficulty to measure the gap width.

SI Movie 3.

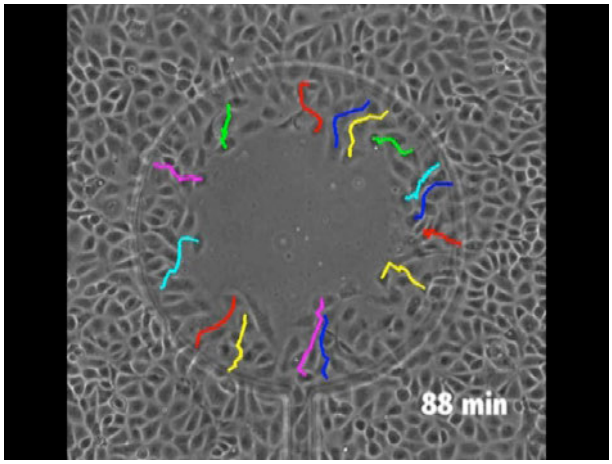

The blank-filling process around a button. The video is generated from a series of phase contrast microscopic images. The positions of a few cells around the edge of the blank are identified in each image and the trajectories of these cells are marked in the video.

SI Movie 4.

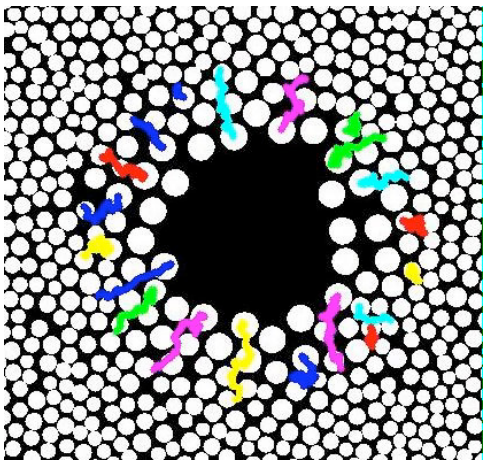

The simulated blank-filling process. During the simulation, each cell will choose its moving direction, or grow, based on a particle model described in the supplementary methods. The positions of a few cells around the edge of the blank are identified in each image and the trajectories of these cells are marked in the video.

SI Movie 5.

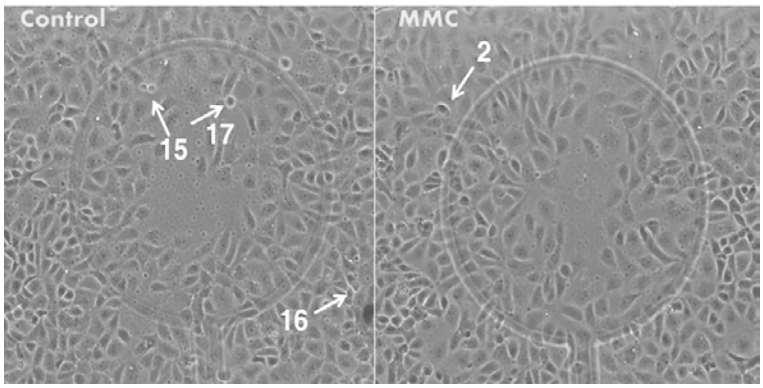

The blank-filling process of HUVECs with and without MMC treatment. Each cell-dividing event within the field of view has been identified and counted. MMC will inhibit cell proliferation, hence less cell dividing events are recorded. We use this method to quantitatively measure the proliferation rate of HUVECs on-chip and notice that with normal culture condition the proliferation will not make significant contribution to the blank-filling with a short experimental time.

SI Movie 6.

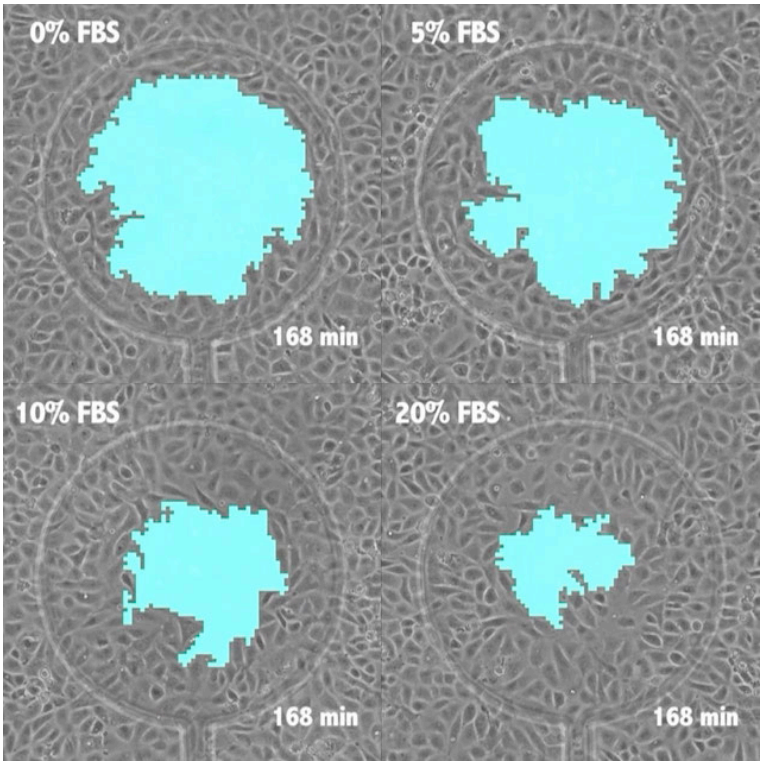

Time-lapse videos of HUVECs on a single chip with different FBS concentration show that the cell motility is affected by the serum concentration.

SI Movie 7.

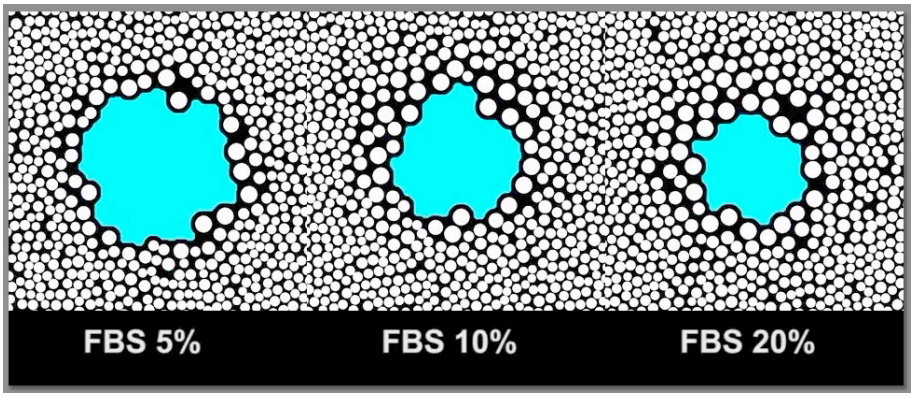

The simulated time-lapse images of cell migration with different motility. These videos are used to fit the experimental data for calculate the cell migration speed of single cells.

Supporting codes for image processing (Matlab script)

```
% the code of "calcuArea .m"
% calcuArea.m calculate the areas of blank units in NUM time-lapse images.
% A median filter is applied to the picture N times.
% THRESH is the threshold for the variance of the intensity to differentiate cell
unit from blank unit.
% SIZE×SIZE pixel sections are cropped from the original time-lapse images for
image processing.
clc;
clear;
%%
N=2; THRESH=16; NUM=5; SIZE=900;
inPic=imread([int2str(1),'.jpg']);          % load the first image of each picture
series.
for k=1:N
   inPic=medfilt2(inPic);              % apply an median filter to the picture N times
end
[Centroid,bwPic]=gray2bwPic(inPic, THRESH);   % transform a grayscale image
to a binary image
showPic(:,:,1)=inPic;                  % display the picture to adjust THRESH
showPic(:,:,2)=inPic+uint8(bwPic*255);
showPic(:,:,3)=inPic+uint8(bwPic*255);
imshow(showPic);
hold on;
plot(Centroid(1),Centroid(2),'*')
clear showPic;

%%
for picNum=1:NUM
  inPic=imread([int2str(picNum),'.jpg']);
     inPic=imcrop(inPic,[Centroid(1)-SIZE/2,Centroid(2)-SIZE/2,SIZE-1,SIZE-1]);
                              % crop SIZE*SIZE pixel sections from the original time-
lapse images
  [serialCentroid,bwPic]=gray2bwPic(inPic, THRESH);
  buttonArea(picNum)=sum(sum(bwPic));
  showPic(:,:,1)=inPic;
  showPic(:,:,2)=inPic+uint8(bwPic*255);
  showPic(:,:,3)=inPic+uint8(bwPic*255);
  imwrite(showPic,[int2str(picNum),'.processed.jpg']);
end
xlswrite(['buttonArea.xls'],[buttonArea]);

% the code of "gray2bwPic .m"
% gray2bwPic.m is a son function of calcuArea.m to transform a grayscale image
to a binary image and calculate the centroid of the blank region.
function [Centroid,bwPic]= gray2bwPic (inPic, threshold)
for i = 1:size(inPic,2)/10
```

```
  for j = 1:size(inPic,1)/10
     h_index = (i-1)*10+1;
     l_index = (j-1)*10+1;
     subPic = double(imcrop(inPic,[h_index,l_index,9,9]));  % divide an original
image into 10×10 pixel units
     tmp = reshape(subPic,10*10,1);
     Variance = var(tmp);          % calculate the intensity variance for each unit
     if Variance < threshold        % use the threshold to determine the unit
belongs to cell region or blank region
        inPic(l_index:l_index+9,h_index:h_index+9) = 1;
     else
                  inPic(l_index:l_index+9,h_index:h_index+9) = 0;
     end
  end
end
bigArea = bwareaopen(inPic,6000,4);     % pick the biggest connected region and
fill all the speckles inside this region as the blank area
bigArea = imfill(bigArea,'holes');
bigArea = bwlabel(bigArea);
picStat = regionprops(bigArea,'Area','Centroid');
for k = 1:max(max(bigArea))
  conArea(k,1) = picStat(k,1).Area;
end
bigAreaIndex = find(conArea==max(conArea));
Centroid = picStat(bigAreaIndex,1).Centroid;
bwPic = bigArea == bigAreaIndex;
```

Note: The input should be an image series containing NUM images with the name '1.jpg', '2.jpg', …'NUM.jpg'. The output are the processed square images cut from the original images with blank regions labeled in cyan and a excel file with the corresponding blank region areas. For example, if the input is 1.jpg, the output will be 1.processed.jpg and buttonArea.xls containing the blank area '249600'.

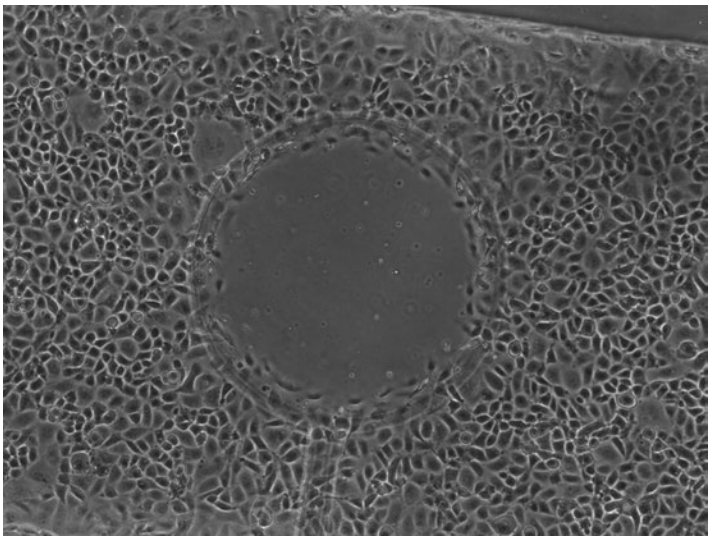

1.jpg

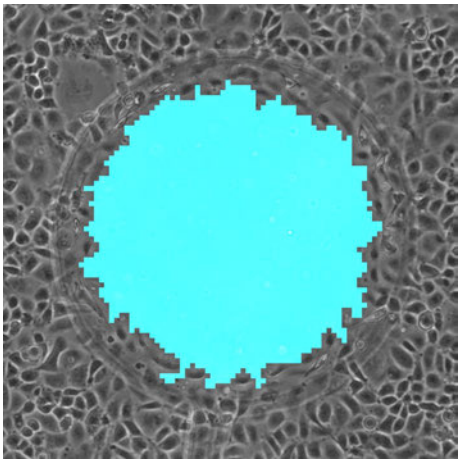

1.process.jpg